Principal Component Analysis Based Hybrid Speckle Noise Reduction Technique for Medical Ultrasound Imaging

Yasser M. Kadah[1]*, Ahmed F. Elnokrashy[2], Ubaid M. Alsaggaf [3], Abou-Bakr M. Youssef [4]
Electrical and Computer Engineering Department, King Abdulaziz University, Jeddah, Saudi Arabia[1, 3]
Electrical Engineering Department, Benha University, Benha, Egypt[2]
Biomedical Engineering Department, Cairo University, Giza, Egypt[1, 4]

***Abstract*—Ultrasound imaging is the safest and most widely used medical imaging technique available today. The main disadvantage of ultrasound imaging is the presence of speckle noise in its images that may obscure pathological changes in the body and makes diagnosis more challenging. Therefore, many techniques were proposed to reduce speckle and improve image quality. Unfortunately, variations of their performance with different scan parameters and due to their methodologies make it hard to choose which one to adopt in clinical practice. In this work, we consider the problem of combining the information from multiple speckle filters and propose the use of principal component analysis to find the optimal set of weights that would retain the most information and hence would better represent the data in the final image. The new technique is implemented to process ultrasound images collected from a research system and the outcomes are compared to the individual techniques and their average using quantitative image quality metrics. The proposed technique has potential for utilization in clinical settings to provide consistently better-quality combined images that may help improve diagnostic accuracy.**

***Keywords*—Image quality metrics; principal component analysis; speckle reduction; ultrasound imaging**

I. Introduction

Ultrasound imaging is one of the most widely used medical imaging techniques available today. It offers a versatile tool for scanning soft tissues and blood flow in the body with applications in abdominal, cardiac, vascular, musculoskeletal, obstetrical and gynecological imaging. Since pulse-echo ultrasound imaging uses weak ultrasonic pulses in human tissues, it is presently considered among the safest medical imaging modalities. It is even allowed to be used for obstetrical applications to assess the health of the fetus. Furthermore, ultrasound imaging systems are available in different forms that include smartphone-based systems or portable scanners that target basic applications such as abdominal imaging and are available at very low cost. They also extend to high-end systems that target specialized applications such as surgical or echocardiographic systems at much higher cost. Therefore, the utility of ultrasound imaging technology extends across the different layers of healthcare delivery to include populations in low-income areas all the way to those receiving care at specialized hospitals. The versatility of ultrasound imaging is expected to lead the technology to become a necessary tool for general practitioners just like the stethoscope.

The main barrier to wider adoption of ultrasound imaging in medicine is the noisy appearance of its output images, which makes the task of reading images more challenging compared to several other modalities [1]. This presence of noise causes problems in the interpretation of ultrasound images particularly when slight pathological variations are present within. Consequently, the problem of image denoising in ultrasound images has been addressed by research from academic and industrial researchers. Improving the quality of ultrasound images by reducing noise is likely to expand its utility and introduction into new applications [2].

In addition to the random noise expected from the electronics used in collecting ultrasound imaging echoes, a deterministic yet unknown type of noise-like texture called speckle noise appears as a direct result of the way ultrasound imaging is performed [3]. Ultrasound imaging works by transmitting an ultrasonic wave burst through the tissues from a probe. This wave travels through the different layers of tissues producing reflected and scattered echoes [4]. The reflection of waves happens when the size of interfaces is larger than the wavelength of ultrasound waves, while scattering happens when the interfaces are significantly smaller than this wavelength [1]. The ultrasound wavelength is less than a millimeter in the frequency range of ultrasound imaging and hence, organ boundaries and walls of large blood vessels produce reflected waves, while small vessels and the cellular matrix within organs produce scattered waves [3][4]. Since such interaction modes depend on the ultrasound transducer shape, frequency and orientation as well as the complex three-dimensional shapes, sizes and organizations of the interfaces within the tissues, the interference pattern of echoes from many interactions results in a pattern of constructive and destructive interferences that appears as a pseudo-random noise in the final image called speckle noise [5]. The speckle noise is different from the random noise encountered from thermal noise in the analog front-end electronics for example in that the speckle pattern remains stationary as long as the imaging conditions are maintained. On the other hand, random noise pattern changes with time and therefore temporal averaging is usually done to reduce its effect on the image [6]. Therefore, speckle reduction cannot be done with temporal averaging and requires fundamentally different approaches to perform [7][24].

*Corresponding Author.

In this work, we consider the problem of combining the information from multiple speckle filters and propose the use of principal component analysis to find the optimal set of weights that would retain the most information and hence would better represent the data in the final image. The new technique is implemented to process ultrasound images acquired from an ultrasound imaging research system and the outcomes are compared to the individual techniques and their average using quantitative image quality metrics. The proposed technique has potential for utilization in clinical settings to provide consistently better-quality combined images that may help improve diagnostic accuracy.

II. Literature Review

Many research studies were performed to address the problem of speckle reduction. Based on their fundamental approach, the research in this area can be generally categorized as being either acquisition-based or postprocessing-based. The acquisition-based approach works by collecting and averaging several images with slightly different imaging parameters such that their speckle patterns are different [1][5][6]. Even though this approach offers an apparently simple solution that takes advantage of the speckle formation physics, it is practically difficult to implement and costly on ultrasound imaging systems and adds constraints on the maximum frame rate that may limit some clinical applications.

On the other hand, the postprocessing-based approach has received more attention from most research groups given that it uses the acquired image without any modifications to the data acquisition method on the ultrasound imaging system. The techniques in this category apply image filtration to suppress speckle noise while trying to maintain the other image features such as the edges. Therefore, a general-purpose digital image processing system with access to the image storage of the ultrasound imaging system can be used to perform its job. As such, it can work on an external computer with a frame grabber or other means to collect ultrasound images from an existing ultrasound imaging system without making any changes to it. With the advances made in computing hardware and software including parallel processing and graphics processing units (GPUs), this approach offers versatile solution that meets practical need to work with existing ultrasound imaging systems.

The existing postprocessing methods can be broadly classified based on their filtration strategy into four distinct classes, with many hybrids across them. Based on how the filtration is done, such methods use linear, nonlinear, physics-based methods like anisotropic diffusion, or wavelet shrinkage filtration [6]. The linear filtration works in the image domain using spatial domain filters and includes such techniques as first-order statistics filtering, local statistics filtering with higher moments, and homogeneous mask area filtering [8][9][10]. The nonlinear filtration is similar to linear filters in being image-based method but the spatial domain filters in this class relies on nonlinear functions such as median filtering, linear scaling filter, geometric filtering, and homomorphic filtering [11][12][13][14]. The physics-based class attempts to utilize simulations of physical phenomena such as diffusion to reach a more homogeneous texture and reduce speckle noise. Examples of this class include anisotropic diffusion filtration and its variants [7][15][16][17][18]. The wavelet shrinkage methods decompose the texture in the wavelet domain and truncation of small coefficients related to speckle noise [19][20][21][22]. Several hybrid methods that combine techniques from two or more of these classes between the above methods were also studied in the literature [23][24].

In spite of the good performance reported by the above speckle reduction methods to improve ultrasound images, there remain major issues that hinder their clinical utility in routine practice. The most important of these is that their performance has wide variability across different techniques and even within the same technique for different ultrasound image characteristics. This makes it difficult to choose one technique to adopt in a particular clinical setting given the wide variability of image characteristics with different selected imaging parameters such as ultrasound frequency, depth, and ultrasound probe geometry. Furthermore, the limited success in combining advantages from different categories of speckle reduction techniques with the present hybrid methods indicates a gap in the research within this area. Therefore, the development of a hybrid technique that would allow for a consistent performance while offering a way of combining image quality advantages from different categories would be highly desired to boost performance in clinical use.

Principal component analysis (PCA) was utilized in ultrasound imaging applications using different approaches. In [25], the authors proposed a speckle reduction method based on the segmentation of the ultrasound image into overlapping regions followed by the application of PCA to the set of segmented regions after reshaping each into a vector. This is similar in principle to the approach in [26] in other image denoising applications where local pixel grouping was used before PCA, and a multistage process is applied iteratively to improve denoising performance. Also, a similar approach was used in [27], where the authors also proposed the use of PCA to denoise multi-frame optical coherence tomography data after dividing them into 3D blocks. In [28], the authors presented a survey of blind source separation applications such as PCA in ultrasound imaging and suggested that it can be used to filter out clutter and noise using spectral thresholding. They pointed out the difficulty to make such techniques work adaptively because of the variations in clutter and noise subspaces across different applications. In [29], the authors proposed an approach for speckle noise suppression in medical ultrasound Images by combining PCA and nonlinear diffusion. In this technique, the PCA is used as an orthogonal transformation to a domain where the nonlinear diffusion is applied after bit plane slicing then the results is transformed back using inverse PCA to form the denoised image. In [30], the authors suggested the use of PCA to reduce the speckle noise in echocardiography frame sequences Using PCA. They reshaped each frame into a vector and performed PCA on the set of vectors obtained from the frame sequence. The resultant PCA underwent a process similar to wavelet shrinkage whereby the subspace components corresponding to small eigenvalues below a certain threshold were omitted and the remaining components were used to reconstruct the denoised image. In

[31], the authors proposed a hybrid of several denoising approaches where PCA is used to combine the outputs of those approaches to obtain the denoised image.

Even though the previous studies included interesting applications of PCA in different aspects of ultrasound imaging, their techniques did not address the problem of optimal combination of information from multiple speckle reduction categories. This problem will be addressed in this work.

III. METHODOLOGY

The received signal in ultrasound imaging can be modeled as the sum of a true signal coming from reflections and scattering from underling tissue interfaces and a superimposed random noise mainly from the electronics used in the analog front-end of the system. The true signal component can be further subdivided into signal from specular reflectors that delineate the major interfaces within the field of view, and another component coming from the summation of many wavelets coming from scatterers resulting in pseudo-random pattern of signal intensities called speckle. Unlike random noise, the speckle pattern depends on the underlying tissue characteristics such as cell sizes and distributions. Therefore, while the random noise changes with every acquisition, the speckle pattern remains the same provided that the same imaging conditions such as location of probe and imaging frequency and transmission focal points remain unchanged.

This study starts by recognizing the fact that there are many present techniques for speckle reductions that perform very well in some applications while others perform better in other applications. Rather than attempting to propose yet another technique, this study searches for a way to develop a hybrid method that combines several techniques in such a way to perform consistently at the peak performance. The research hypothesis is that using techniques from different speckle reduction categories combined using a technique that minimizes information loss such as principal component analysis would achieve that goal.

From the theory of principal component analysis technique, the first principal component is a smart way of representing the information present in a set of data vectors (or observations) whereby a set of weights are calculated such that it adaptively and optimally retains more information from the original data vectors than any other combination [36]. For example, in theory, the first principal component allows better representation of the original data than simple combination with equal weights as in averaging. This is the basis for our new method to combine data from different speckle reduction filters. In particular, four popular speckle reduction filtering techniques as examples from the four main postprocessing categories (without loss of generality) are used along with the original image as the input to the principal component analysis to find the optimal way of combining their information. These techniques are wavelet shrinkage [19][21], relaxed median (RMedian) filtering [13][14], speckle reducing anisotropic diffusion (SRAD) [15][16][17], and local statistics based filtering (Lee) [8][9]. The implementation parameters were used as in the most recent variant in each technique.

The details of the new methodology are as follows. Ultrasound images are collected as a set of lines (or sticks) that span the scanned region in a linear or a sector manner depending on the imaging probe used. The resulting data are called the stick data and are used to form the properly formatted output image by the image reconstruction technique given the scanning parameters and geometry information. The use of stick data rather than image lines maintains all data points independent by avoiding point correlations from interpolation operations. They also help reduce the computational cost of applying different processing methods on the data. The new technique is implemented by forming a matrix containing the set of vectors with the original data and four filtered versions and use PCA to find the optimal weights to combine them.

Let the original stick data image be $f(m,n)$ of size $M\times N$. The original stick data image is processed using four speckle filtering techniques, namely, wavelet, relaxed median, SRAD and Lee filters. The outcomes from these four filters will be $f_W(m,n)$, $f_R(m,n)$, $f_S(m,n)$ and $f_L(m,n)$ respectively. The observations data matrix D is composed by reformatting the original and four processed stick data images of size $M\times N$ into $MN\times 1$ column vectors, $F, F_W, F_R, F_S,$ and F_L, where each is placed as a column in the D matrix of size $MN\times 5$.

$$\mathrm{D} = [F \mid F_W \mid F_R \mid F_S \mid F_L]. \quad (1)$$

The covariance matrix $\mathrm{COV_D}$ of size 5×5 is estimated as,

$$\mathrm{COV_D} = \left[\, \hat{F} \mid \hat{F}_W \mid \hat{F}_R \mid \hat{F}_S \mid \hat{F}_L \,\right]^T . \left[\, \hat{F} \mid \hat{F}_W \mid \hat{F}_R \mid \hat{F}_S \mid \hat{F}_L \,\right], \quad (2)$$

where $\hat{F},\ \hat{F}_W, \hat{F}_R, \hat{F}_S\ and\ \hat{F}_L$ are the centered versions of their original vectors after subtracting their mean values. Then, the principal component analysis is performed on $\mathrm{COV_D}$ to obtain the vector of coefficients W_{PC} of the principal component (that is, the eigenvector for the largest eigenvalue of the covariance matrix). The reformatted column vector G of size $MN\times 1$ representing the final processed stick data image $g(m,n)$ of size $M\times N$ is then computed as the weighted average of all images as,

$$G = \frac{\mathrm{D}\cdot W_{PC}}{\mathrm{sum}\,(W_{PC})}. \quad (3)$$

Here, $\mathrm{sum}\,(W_{PC})$ is the summation of W_{PC} vector components to ensure that the weighted average weights add to unity. The final processed stick data image $g(m,n)$ of size $M\times N$ is obtained by reformatting G and is sent to image reconstruction to generate the final display image. A block diagram of the new method is presented in Fig. 1.

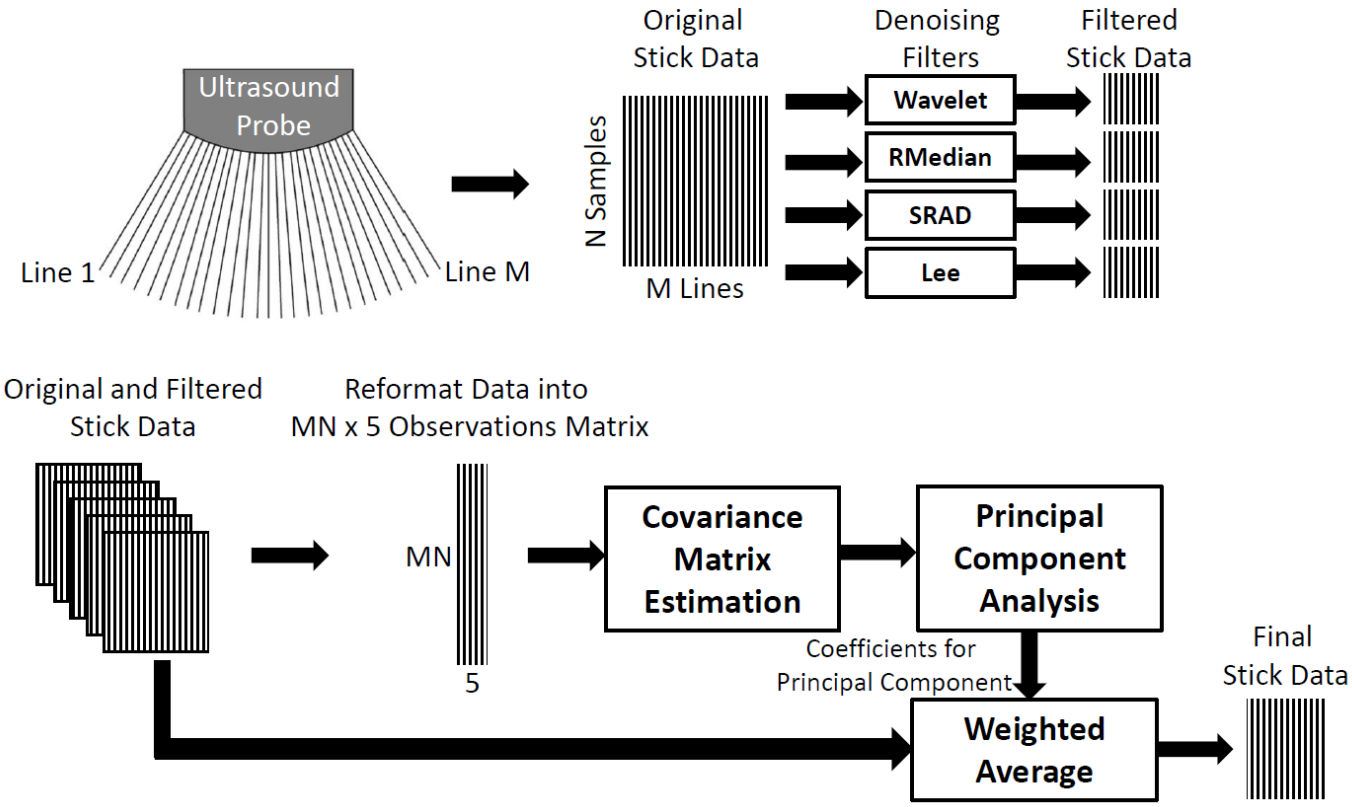

Fig. 1. Diagram showing the steps of the new technique whereby original stick data and its filtered versions multiple speckle reduction techniques undergo PCA to estimate the best weights to combine them for best information retention.

To compare the results between the new technique and averaging in a quantitative manner, several image quality metrics are used to assess the outputs from both techniques as they were applied to several data sets acquired using different imaging conditions (for example, different probes and different applications). The image quality metrics used are root mean squared error [6], Laplacian mean squared error [32], Minkowski error metric [33], structural similarity index (SSIN) [33], , universal quality index (Q) [33][34], signal-to-noise ratio (SNR) and peak signal-to-noise ratio (PSNR) [35]. This allows for objective assessment of the results. The detailed mathematical definitions of such metrics are as follows.

The root mean squared error (RMSE) is the square root of the average of the squared error over the whole image. It is generally considered as an approximation of the standard error.

$$RMSE = \sqrt{\frac{1}{MN}\sum_{m=1}^{M}\sum_{n=1}^{N}(g(m,n) - f(m,n))^2}\,. \quad (4)$$

The Laplacian mean squared error (LMSE) is the squared error between the Laplacian of the original and processed images averaged over the entire image. It generally assesses the edge preservation in the processing algorithm. A better-quality processed image will have a lower RMSE value.

$$LMSE = \frac{1}{MN}\sum_{m=1}^{M}\sum_{n=1}^{N}(g_L(m,n) - f_L(m,n))^2\,, \quad (5)$$

where $g_L(m,n)$ and $f_L(m,n)$ are the Laplacians of the processed and original images respectively. A better-quality processed image will have a lower LMSE value.

The Minkowski error metric computes the norm of the difference between the original and processed images using different vector norms. The equation for β-norm Minkowski error metric is given as,

$$ErrorM(\beta) = \sqrt[\beta]{\frac{1}{MN}\sum_{m=1}^{M}\sum_{n=1}^{N}|g(m,n) - f(m,n)|^{\beta}}\,. \quad (6)$$

Here, we compute the Minkowski error metrics for β values of 3 (ErrorM3) and 4 (ErrorM4). A better-quality processed image will have lower ErrorM3 and ErrorM4 values.

The signal-to-noise ratio (SNR) is an important measure of how the processed signal improved in suppressing noise. A better-quality processed image will have a higher SNR value.

$$SNR = 10\log_{10}\left(\frac{\sum_{m=1}^{M}\sum_{n=1}^{N}(g^2(m,n) - f^2(m,n))}{\sum_{m=1}^{M}\sum_{n=1}^{N}(g(m,n) - f(m,n))^2}\right). \quad (7)$$

The peak signal-to-noise ratio (PSNR) measures the resemblance of the processed image and the original image. A better-quality processed image will have a higher PSNR value.

$$PSNR = -10\log_{10}\left(\frac{RMSE^2}{\max\{f(m,n)\}}\right), \quad (8)$$

where $\max\{f(m,n)\}$ is the maximum intensity value in the original image.

The universal quality index (Q) models any distortion as a combination of three different factors, which are loss of correlation, luminance distortion, and contrast distortion.

$$Q = \frac{\sigma_{gf}}{\sigma_g \sigma_f} \cdot \frac{2\bar{f}\bar{g}}{\bar{f}^2+\bar{g}^2} \cdot \frac{2\sigma_g \sigma_f}{{\sigma_g}^2+{\sigma_f}^2} \ , \quad (9)$$

where $\bar{f}$ and $\bar{g}$ are mean values of the original and processed images respectively with their standard deviations σ_f and σ_g . Also, σ_{gf} represents the covariance between the original and processed images. A better-quality processed image will have a higher Q value.

The structural similarity index (SSIN) between the original and processed images is a more general form of Q developed by the same research group. A higher value of SSIN indicates a higher quality processed image.

$$SSIN = \frac{(2\bar{f}\bar{g}+c_1)}{(\bar{f}^2+\bar{g}^2+c_1)} \cdot \frac{(2\sigma_{gf}+c_2)}{({\sigma_g}^2+{\sigma_f}^2+c_2)} \ , \quad (10)$$

where c_1 and c_2 are constants computed as 0.01 and 0.03 of maximum value in image dynamic range respectively (255 in the case of ultrasound images).

IV. Experimental Setup and Data Collection

The experimental ultrasound imaging data were acquired using an ultrasound imaging research system (Digison Digital Ultrasound Research system, Mashreq., Egypt) [38]. A customized research interface was used to set all imaging parameters and allowed the acquisition and storage of raw data samples at high sampling rates of 50 M Samples/s at a quantization of 16 bits. To ensure that the collected data set includes diverse image characteristics, imaging experiments were performed using several multifrequency ultrasound transducers including different linear and convex array probes including an endo-cavity probe. Furthermore, the experiments included different clinical applications on human volunteers and scanning of a tissue-mimicking quality assurance phantom (CIRS Inc., U.S.A.). A total of 10 images were collected for each experiment to do temporal averaging to remove present random noise. The complete data set included the results from 26 different imaging experiments with a total of 260 images. Fig. 2 demonstrates a sample image from each of the 26 imaging experiments to show the wide variation in their nature and characteristics. The conventional ultrasound signal processing stack was used to perform peak detection using Hilbert transformation then resampling to reduce the number of samples in each line to 512. The number of acquired lines for each imaging experiment was 128 and this 128×512 data array of resampled line data was called the stick data. The new technique was applied on the stick data to obtain the final processed image. The final image reconstruction from the processed stick data was subsequently performed to obtain the final processed images. The new methodology was implemented using Matlab 2022b (Mathworks Inc., U.S.A.). The data processing system was a desktop computer with 11th generation Intel® Core™ i7 processor and 32 GB of RAM running a 64-bit Windows 11 Home Edition operating system.

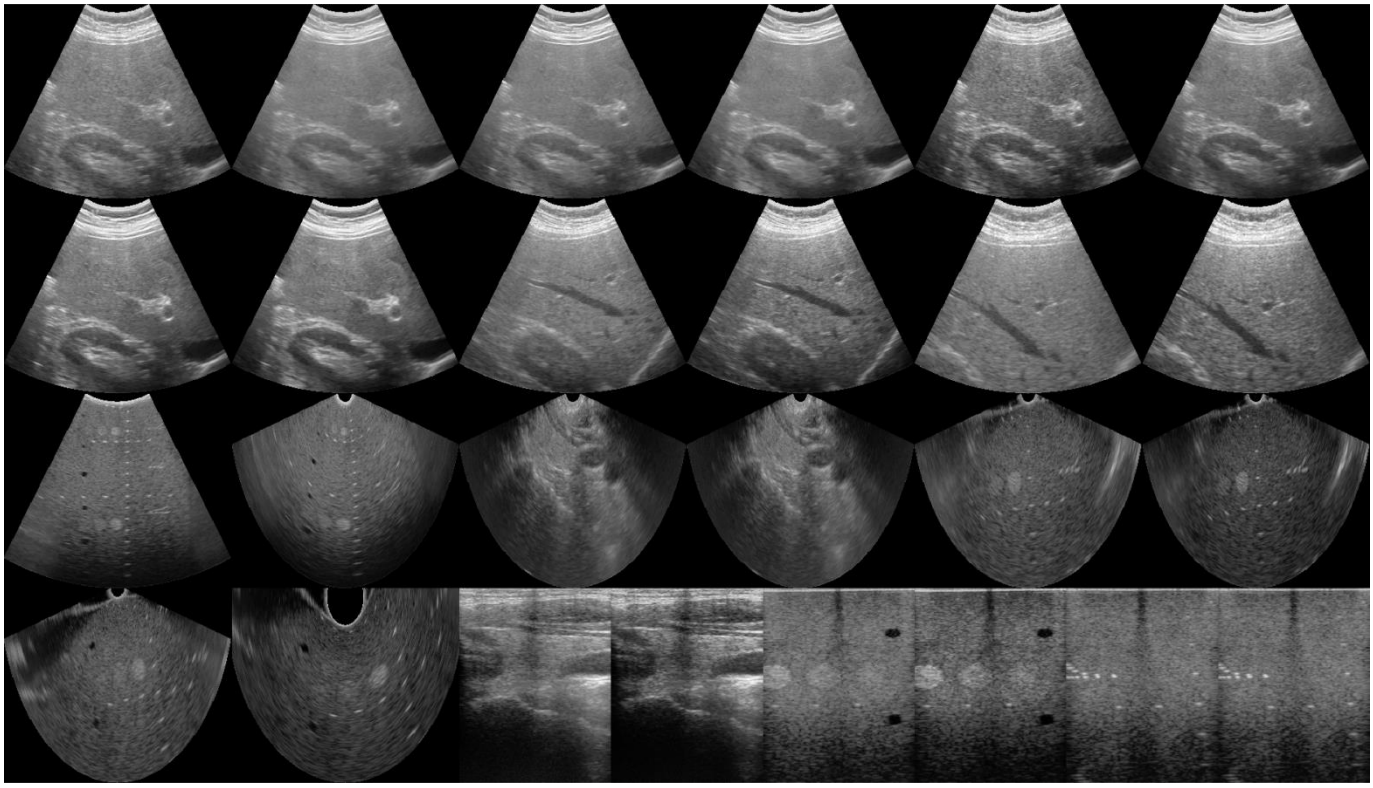

Fig. 2. Illustration of the different imaging experiments performed in this study.

V. Results and Discussion

Example qualitative results of applying the new methodology compared to the original images and the results from individual speckle reduction filters as well as their average are shown in Fig. 3. To better demonstrate the performance, the results from imaging experiments using three different probe geometries were included for both the tissue-mimicking phantom and real human scans. The qualitative evaluation can be done by observing the smoothness of speckle texture as well as the sharpness or definition of edges in each image as compared to the original. As can be observed, variations in both are found across the results from the individual speckle reduction filters where better smoothness comes at the cost of blurry edges such as with the Lee filter results. This can be seen more clearly in the results from phantom experiments given the structure of the phantom. In the results from all image experiments, the proposed PCA-based hybrid technique offers smoothness and edge definition that is comparable to the best of all individual techniques. Furthermore, the results from the simple average of individual techniques appear to partially inherit the quality issue such as blurring more prominently than the new technique.

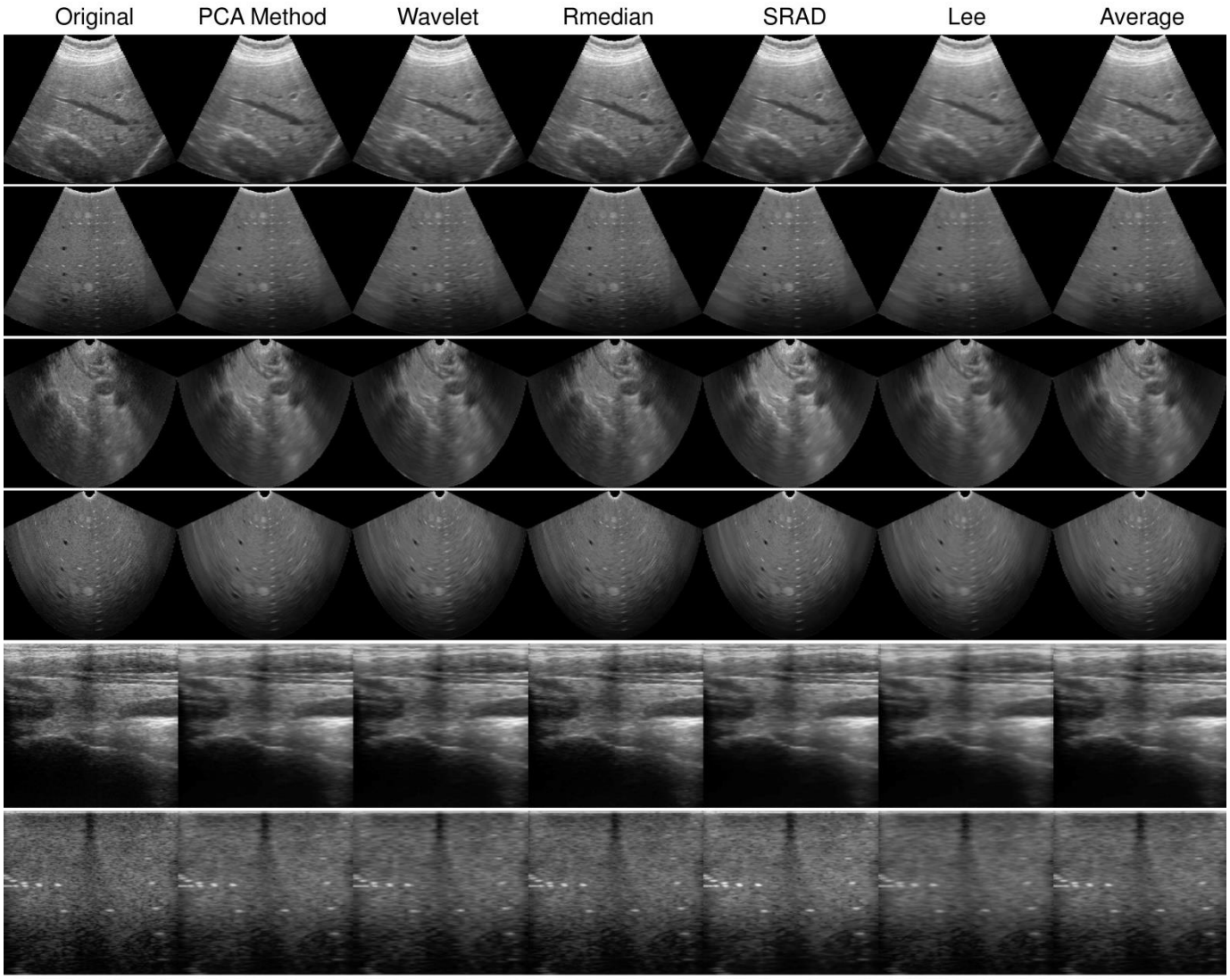

Fig. 3. Experimental results from the new technique are compared to those from the individual techniques used in addition to their average. the results are provided for different probe geometries and scan parameters from both a tissue-mimicking phantom and human volunteers.

The quantitative evaluations of the results are provided in Table I, which presents the percentage mean change in image quality metrics compared to the new PCA-based hybrid technique along with its standard deviation and p-value of statistical significance over the set of 26 experiments. For each metric, the percentage mean change of a particular technique is calculated as the average of the difference between the metric values of that particular technique and the new PCA-based hybrid technique, divided by the average of that metric for the new PCA-based hybrid technique. This formula was chosen to make the percentage change always relative to the same quantity across different techniques to make consistent comparisons. For better inspection of the results, the image quality metrics were grouped into either error or quality metrics as shown in the first column. When a technique has a positive percentage mean change in the error metrics, this means that its error metric is higher than that of the new technique, which would indicate lower performance. ON the other hand, a lower performance in the quality metrics is when a technique has a negative percentage mean change in the error metrics, which means that its quality metric is lower than that of the new technique. As can be observed, the results indicate that the new PCA-based hybrid technique offers better performance across all metrics with varying degrees. For example, in the universal quality index that deterioration varies from -2.77% for relaxed median filter to -30.55% for wavelet filter. It should be noted that the other metrics for these same techniques were very different where for example they were higher by 107.84% and 97.9% respectively for Laplacian mean squared error. This generally demonstrates the issue of variable performance of individual techniques across metrics where some perform better on quality and others on error metrics. One final observation is that the performance of the new PCA-based hybrid technique was consistently superior to that of the average of individual techniques, with significantly higher improvements in error metrics than quality metrics.

In order to ensure that the detected mean changes are statistically significant, a two-sample student t-test was applied and the p-values are listed in the same bin as the percentage mean change in Table I. A significance level of 0.05 was used and higher p-values where statistical significance cannot be confirmed at that level were denoted with "*" in the table. As can be observed, only three results were not statistically significant and they were all for the relaxed median filter. All results for the average of individual techniques were statistically significant indicating that there is a real performance boost. The overall results generally support the research hypothesis that the performance of the new PCA-based hybrid technique is better than or not different from the best individual technique.

TABLE I. PERCENTAGE MEAN CHANGE IN IMAGE QUALITY METRICS COMPARED TO THE NEW PCA-BASED HYBRID TECHNIQUE ALONG WITH ITS STANDARD DEVIATION AND P-VALUE OF STATISTICAL SIGNIFICANCE OVER THE SET OF 26 EXPERIMENTS

Assessment Metric		Wavelet	RMedian	SRAD	Lee	Average
Error Metrics	Root Mean Squared Error (RMSE)	+49.44% ± 14.66 (p<0.001)	+6.69% ± 12.69 (p=0.103*)	+93.25% ± 70.71 (p<0.001)	+46.78% ± 14.33 (p<0.001)	+23.84% ± 3.1 (p<0.001)
	Laplacian Mean Squared Error (LMSE)	+107.84% ± 14.73 (p<0.001)	+97.9% ± 18.9 (p<0.001)	+26.83% ± 17.21 (p<0.001)	+98.31% ± 14.86 (p<0.001)	+58.72% ± 4.51 (p<0.001)
	Minkowski Error Metric (β=3) (ErrorM3)	+49.36% ± 13.32 (p<0.001)	+29.18% ± 12.67 (p<0.001)	+76.49% ± 59.56 (p<0.001)	+49.99% ± 15.05 (p<0.001)	+24.34% ± 2.94 (p<0.001)
	Minkowski Error Metric (β=4) (ErrorM4)	+49.6% ± 12.81 (p<0.001)	+71.18% ± 18.17 (p<0.001)	+64.0% ± 52.31 (p<0.001)	+52.93% ± 15.67 (p<0.001)	+24.82% ± 2.88 (p<0.001)
Quality Metrics	Signal-to-Noise Ratio (SNR)	-12.95% ± 3.1 (p<0.001)	-2.04% ± 3.78 (p=0.471*)	-18.34% ± 10.3 (p<0.001)	-12.56% ± 3.17 (p<0.001)	-6.86% ± 0.67 (p<0.001)
	Peak Signal-to-Noise Ratio (PSNR)	-10.38% ± 3.2 (p<0.001)	-2.31% ± 4.17 (p=0.166*)	-14.44% ± 8.24 (p<0.001)	-11.52% ± 3.0 (p<0.001)	-6.14% ± 0.62 (p<0.001)
	Structural Similarity Index (SSIN)	-23.59% ± 6.34 (p<0.001)	-2.5% ± 4.16 (p=0.013)	-5.84% ± 3.86 (p<0.001)	-23.56% ± 3.75 (p<0.001)	-10.21% ± 1.5 (p<0.001)
	Universal Quality Index (Q)	-30.55% ± 5.95 (p<0.001)	-2.73% ± 5.11 (p=0.027)	-9.88% ± 7.1 (p<0.001)	-31.24% ± 3.4 (p<0.001)	-13.93% ± 1.95 (p<0.001)

* Not statistically significanct.

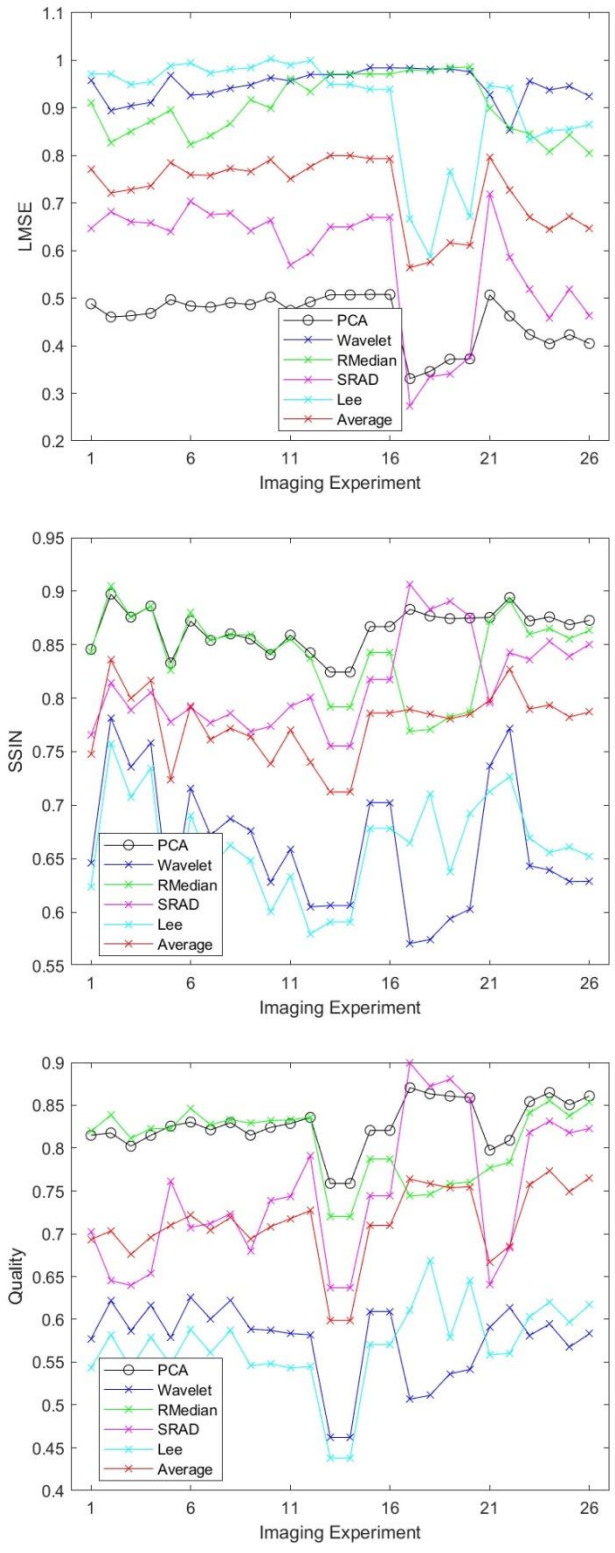

Fig. 4. Experimental results showing example quality metrics Laplacian Mean Squared Error (LMSE), structural similarity index (ssin), and universal quality index (Q) for 26 imaging experiments.

In order to illustrate the variability of metric values across different imaging experiments, Fig. 4 presents the values of Laplacian mean squared error, structural similarity index and universal quality metrics for each of the 26 imaging experiments. It can be observed that the different techniques have significant variability when applied to different experiments with different probe geometry and scan parameters. Furthermore, it is evident that the performance of the new PCA-based hybrid technique is better than or equal to the best individual technique in the majority of experiments, which again confirms the validity of the research hypothesis of developing this method. It can be also observed that the results from the average of individual techniques always lie in the middle of all individual techniques. This means that it may be considered as a way of obtaining consistent results from all techniques, but its performance will not be the best.

In order to verify the importance of including the original image in the observations matrix along with those from the speckle filters, the new technique was implemented with only 4 columns in the observations matrix D by excluding the original image. The quantitative evaluations of the results are presented in Table II. As can be observed, the obtained outcome has mixed performance across each metric as evident by the mixed negative and positive values in each. This indicates the results of excluding the original image are significantly worse than with the original image included. Furthermore, the results of excluding the original image appear to be very close to those of the average of individual techniques. This is evident from the small percentage mean differences and from the fact that there is no statistically significant difference between applying the new method with excluding the original image and that of the average of individual techniques. This indicates the important role of the information in the original image in guiding the estimation of weights used to combine it with the different individual techniques. To demonstrate this further, the computed weights for all experiments are shown in Fig. 5. As can be seen, the weights vary significantly across imaging experiments, which outlines the importance of their adaptive estimation. The weights for the original image were second highest in the majority of experiments indicating its importance in the outcome.

With the performance advantage of the PCA-based hybrid technique established by the results, the main challenge for its widespread application appears to be mainly computational. Rather than using an individual speckle filter, four filters need to be applied in the new method. The computations needed to perform the new technique can be divided into the computations needed for the speckle filters (which may vary with implementation), covariance matrix estimation, principal component analysis of a 5×5 matrix, the weighted average of 5 stick data images. Nevertheless, this computational cost can be considered reasonable for real-time performance especially with current high processing power available in modern digital ultrasound imaging systems. Furthermore, since we require only the first eigenvector corresponding to the maximum eigenvalue, significantly faster solvers can be utilized [37].

TABLE II. PERCENTAGE MEAN CHANGE IN IMAGE QUALITY METRICS COMPARED TO THE NEW PCA-BASED HYBRID TECHNIQUE WITHOUT INCLUDING ORIGINAL IMAGE IN OBSERVATIONS MATRIX ALONG WITH ITS STANDARD DEVIATION AND P-VALUE OF STATISTICAL SIGNIFICANCE OVER THE SET OF 26 EXPERIMENTS

	Assessment Metrics	Wavelet	RMedian	SRAD	Lee	Average
Error Metrics	Root Mean Squared Error (RMSE)	+19.43% ± 10.97 (p<0.001)	-14.73% ± 10.44 (p<0.001)	+54.44% ± 55.67 (p=0.002)	+17.31% ± 11.7 (p<0.001)	-1.03% ± 1.91 (p=0.756*)
	Laplacian Mean Squared Error (LMSE)	+32.7% ± 13.07 (p<0.001)	+26.36% ± 15.07 (p<0.001)	-19.02% ± 7.84 (p<0.001)	+26.62% ± 7.11 (p<0.001)	+1.34% ± 1.37 (p=0.66*)
	Minkowski Error Metric (β=3) (ErrorM3)	+19.36% ± 9.73 (p<0.001)	+3.23% ± 10.38 (p=0.337*)	+41.04% ± 47.03 (p<0.001)	+19.86% ± 12.44 (p<0.001)	-0.64% ± 1.51 (p=0.837*)
	Minkowski Error Metric (β=4) (ErrorM4)	+19.54% ± 9.34 (p<0.001)	+36.78% ± 15.58 (p<0.001)	+31.05% ± 41.5 (p=0.001)	+22.2% ± 13.03 (p<0.001)	-0.26% ± 1.19 (p=0.932*)
Quality Metrics	Signal-to-Noise Ratio (SNR)	-6.26% ± 3.26 (p=0.035)	+5.48% ± 4.01 (p=0.075*)	-12.07% ± 11.2 (p=0.002)	-5.85% ± 3.29 (p=0.022)	+0.29% ± 0.57 (p=0.913*)
	Peak Signal-to-Noise Ratio (PSNR)	-4.35% ± 3.26 (p=0.011)	+4.27% ± 4.29 (p=0.018)	-8.69% ± 8.91 (p=0.001)	-5.56% ± 3.17 (p<0.001)	+0.17% ± 0.47 (p=0.899*)
	Structural Similarity Index (SSIN)	-15.31% ± 6.65 (p<0.001)	+8.06% ± 4.95 (p<0.001)	+4.36% ± 4.33 (p=0.002)	-15.28% ± 3.04 (p<0.001)	-0.48% ± 0.53 (p=0.673*)
	Universal Quality Index (Q)	-19.8% ± 8.09 (p<0.001)	+12.33% ± 7.14 (p<0.001)	+4.07% ± 6.54 (p=0.128*)	-20.6% ± 3.22 (p<0.001)	-0.6% ± 0.68 (p=0.737*)

* Not statistically significanct

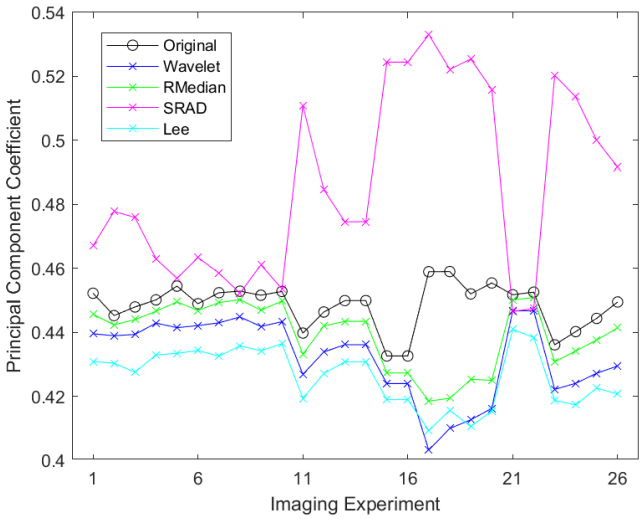

Fig. 5. Illustration of the variations of experimental optimal weights of different images obtained using PCA for the 26 imaging experiments.

VI. CONCLUSIONS

In this study, the combination of information from multiple speckle filters is considered and the use of principal component analysis is proposed to find the optimal set of weights that would retain the most information and hence would better represent the data in the final image. The new technique is implemented to process ultrasound images acquired from a research system and the outcomes are compared to the individual techniques and their average using quantitative image quality metrics. The results confirm that the new PCA-based hybrid technique offers consistent high performance across different experiments. The proposed technique has potential for utilization in clinical settings to provide consistently better-quality combined images that may help improve diagnostic accuracy.

ACKNOWLEDGMENT

This project was funded by the Center of Excellence in Intelligent Engineering Systems (CEIES), King Abdulaziz University, Jeddah, under Grant No. (CEIES-16-07-01). The authors, therefore, acknowledge the technical and financial support of King Abdulaziz University.

REFERENCES

[1] P. R. Hoskins, K. Martin, A. Thrush, Diagnostic Ultrasound: Physics and Equipment, 2nd ed., Cambridge University Press, 2010.

[2] E. Krupinski, H. Kundel, P. Judy, C. Nodine, "The medical image perception society, key issues for image perception research," Radiology, vol. 209, pp. 611–612, 1998.

[3] C. B. Burckhardt, "Speckle in ultrasound B-mode scans," IEEE Trans. Sonics Ultrasonics, vol. SU-25, no. 1, pp. 1–6, 1978.

[4] R. F. Wagner, S. W. Smith, J. M. Sandrik, H. Lopez, "Statistics of speckle in ultrasound B-scans," IEEE Trans. Sonics Ultrasonics, vol. 30, pp. 156–163, 1983.

[5] A. Perperidis, D. Cusack, A. White, N. McDicken, T. MacGillivray, T. Anderson, "Temporal Compounding: A Novel Implementation and Its Impact on Quality and Diagnostic Value in Echocardiography," Ultrasound in Medicine & Biology, vol. 41, no. 6, pp. 1749-1765, 2015.

[6] C. P. Loizou, C. S. Pattichis, Despeckle Filtering for Ultrasound Imaging and Video, Volume I: Algorithms and Software, 2nd ed., Morgan & Claypool, 2015.

[7] K. Z. Abdel-Monem, A. M. Youssef, Y. M. Kadah, "Real-time speckle reduction and coherence enhancement in ultrasound imaging via nonlinear anisotropic diffusion," IEEE Trans. Biomed Eng, vol. 49, no. 9, pp. 997-1014, Sept. 2002.

[8] J. S. Lee, "Digital image enhancement and noise filtering by using local statistics," IEEE Trans. Pattern Anal. Mach. Intell., PAMI-2, no. 2, pp. 165–168, 1980.

[9] O. Rubel, V. Lukin, A. Rubel, K. Egiazarian, "Selection of lee filter window size based on despeckling efficiency prediction for sentinel SAR images," Remote Sensing, vol. 13, no. 10, p.1887, 2021.

[10] A. F. de Araujo, C. E. Constantinou, J. Tavares, "Smoothing of ultrasound images using a new selective average filter," Expert Systems with Applications, vol. 60, pp. 96-106, 2016.

[11] J. Saniie, T. Wang, N. Bilgutay, "Analysis of homomorphic processing for ultrasonic grain signal characterization," IEEE Trans. Ultrason. Ferroelectr. Freq. Control, vol. 3, pp. 365–375, 1989.

[12] M. A. Gungor, I. Karagoz, "The homogeneity map method for speckle reduction in diagnostic ultrasound images," Measurement, vol. 68, pp. 100-110, 2015.

[13] A. B. Hamza, P. L. Luque-Escamilla, J. Martínez-Aroza, R. Román-Roldán, "Removing noise and preserving details with relaxed median filters," Journal of mathematical imaging and vision, vol. 11, no. 2, pp.161-177, 1999.

[14] K. Chauhan, R. K. Chauhan, A. Saini, "Enhancement and Despeckling of Echocardiographic Images," In Soft Computing Based Medical Image Analysis, Academic Press, pp. 61-79, 2018.

[15] P. Perona, J. Malik, "Scale-space and edge detection using anisotropic diffusion," IEEE Trans. Pattern Anal. Mach. Intell., vol. 12, no. 7, pp. 629–639, July 1990.

[16] Y. Yongjian, S. T. Acton, "Speckle reducing anisotropic diffusion," IEEE Trans. Image Process., vol. 11, no. 11, pp. 1260–1270, November 2002.

[17] H. Choi, J. Jeong, "Speckle noise reduction for ultrasound images by using speckle reducing anisotropic diffusion and Bayes threshold," Journal of X-ray Science and Technology, vol. 27, no. 5, pp.885-898, 2019.

[18] R. G. Dantas, E. T. Costa, "Ultrasound speckle reduction using modified gabor filters," IEEE Trans Ultrason Ferroelec Freq Cont, vol. 54, no. 3, pp. 530-538, 2007.

[19] D. L. Donoho, "Denoising by soft thresholding," IEEE Trans. Inform. Theory, vol. 41, pp. 613–627, 1995.

[20] S. Gupta, R. C. Chauhan, S. C. Sexana, "Wavelet-based statistical approach for speckle reduction in medical ultrasound images," Med Biol Eng Comput, vol. 42, pp. 189–192, 2004

[21] A. K. Bedi, R. K. Sunkaria, "Ultrasound speckle reduction using adaptive wavelet thresholding," Multidimensional Systems and Signal Processing, vol. 33, no. 2, pp.275-300, 2022.

[22] J. Kang, J. Y. Lee, Y. Yoo, "A new feature-enhanced speckle reduction method based on multiscale analysis for ultrasound B-mode imaging," IEEE Trans Biomed Eng, vol. 63, no. 6, pp. 1178 – 1191, 2016.

[23] J. Zhang, G. Lin, L. Wu, C. Wang, Y. Cheng, "Wavelet and fast bilateral filter based de-speckling method for medical ultrasound images," Biomed Sig Proc Cont, vol. 18, pp. 1-10, 2015.

[24] Z. A. Mustafa, B. A. Abrahim, I. A. Yassine, N. Zayed, Y. M. Kadah, "Wavelet Domain Bilateral Filtering with Subband Mixing for Magnetic Resonance Image Enhancement," J Med Imag Health Inform, vol. 2, pp. 230-237, 2012.

[25] J. F. Al-Asad, A. M. Reza, U. Techavipoo, "An ultrasound image despeckling approach based on principle component analysis," International Journal of Image Processing (IJIP), vol. 8, no. 4, pp. 156-77, 2014.

[26] L. Zhang, W. Dong, D. Zhang, G. Shi, "Two-stage image denoising by principal component analysis with local pixel grouping," Pattern recognition, vol. 43, no. 4, pp. 1531-49, 2010.

[27] H. Lv, S. Fu, C. Zhang, L. Zhai, "Speckle noise reduction of multi-frame optical coherence tomography data using multi-linear principal component analysis," Optics Express, vol. 26, no. 9, pp. 11804-18, 2018.

[28] R. R. Wildeboer, F. Sammali, R. J. Van Sloun, Y. Huang, P. Chen, M. Bruce, C. Rabotti, S. Shulepov, G. Salomon, B. C. Schoot, H. Wijkstra, "Blind source separation for clutter and noise suppression in ultrasound imaging: Review for different applications," IEEE Transactions on Ultrasonics, Ferroelectrics, and Frequency Control, vol. 67, no. 8, pp. 1497-512, 2020.

[29] M. M. Rahman, P. M. Kumar, M. G. Arefin, M. S. Uddin, "Speckle noise reduction from ultrasound images using principal component analysis with bit plane slicing and nonlinear diffusion method," Proc. 15th International Conference on Computer and Information Technology (ICCIT), pp. 159-163, 2012.

[30] M. Jalali, H. Behnam, P. Gifani, Z. A. Sani, "Simultaneous speckle reduction of echocardiography frame sequence using PCA," Proc. 22nd Iranian Conference on Electrical Engineering (ICEE), pp. 1863-1867, 2014.

[31] I. Kumar, H. S. Bhadauria, J. Virmani, J. Rawat, "Reduction of speckle noise from medical images using principal component analysis image fusion," Proc. 9th International Conference on Industrial and Information Systems (ICIIS), pp. 1-6, 2014.

[32] A. M. Eskicioglu, P.S. Fisher, "Image quality measures and their performance," IEEE Trans. On Communications, vol. 43, no. 12, pp. 2959-2965, 1995.

[33] Z. Wang, A. Bovik, H. Sheikh, and E. Simoncelli, "Image quality assessment: From error measurement to structural similarity," IEEE Trans. Image Process., vol. 13, no. 4, pp. 600–612, April 2004.

[34] Z. Wang and A. Bovik, "A universal quality index," IEEE Signal Process. Lett., vol. 9, no. 3, pp. 81–84, March 2002.

[35] D. Sakrison, "On the role of observer and a distortion measure in image transmission," IEEE Trans. Comm., vol. 25, pp. 1251–1267, November 1977.

[36] R. Bro, A. K. Smilde, "Principal component analysis," Analytical Methods, vol. 6, no. 9, pp. 2812-31, 2014.

[37] G. H. Golub, C. F. Van Loan, Matrix computations, 3rd ed., Johns Hopkins University Press, 2013.

[38] Y. M. Kadah, A. F. Elnokrashy, U. M. Alsaggaf, A. M. Youssef, "Speckle reduction in medical ultrasound imaging based on visual perception model," International Journal of Advanced Computer Science and Applications (IJACSA), vol. 13, no. 11, pp. 575–581, 2022.